PHYSICAL REVIEW B VOLUME 36, NUMBER 15 15 NOVEMBER 1987-II

Exciton binding energies from an envelope-function analysis of data on narrow quantum wells of integral monolayer widths in $Al_{0.4}Ga_{0.6}As/GaAs$

D. F. Nelson, R. C. Miller, C. W. Tu, and S. K. Sputz
AT&T Bell Laboratories Murray Hill, New Jersey 07974
(Received 22 May 1987)

Heavy- and light-hole exciton transitions were observed from isolated quantum wells in two wafers of $Al_{0.4}Ga_{0.6}As/GaAs$ produced by molecular-beam epitaxy using interrupted growth at the heterointerfaces. The transitions can be assigned to well widths that are integral multiples of a GaAs monolayer width with the integers between 6 and 25. Direct measurements of the barrier-layer band gap and barrier-layer exciton binding energy were also made. A detailed envelope-function analysis of this unique data set revealed the necessity of using a soft-edge potential well rather than a square well when analyzing such narrow wells. A reduction in exciton binding energies of 2.5 meV from free charge arising from unintentional barrier doping of $\sim 1\times 10^{14}$ cm^{-3} was found. Exciton binding energies for wells between 17 and 70 Å are deduced from the analysis.

I. INTRODUCTION

Interruption of growth by molecular-beam epitaxy at the interfaces of $Al_xGa_{1-x}As/GaAs$ heterostructures can produce very narrow quantum wells having widths that are uniform over lateral distances ranging from 0.6 to 1.5 μm and that are equal to integral numbers of monolayers of GaAs.[1,2] These conclusions resulted from photoluminescence and excitation spectroscopy observations of heavy- and light-hole excitons confined in such wells. The exciton transitions had spectral widths corresponding to fluctuations of a small fraction of a monolayer width and spectral spacings indicating that they originated from different portions of the wells whose widths differ by integral multiples N of one monolayer thickness. Once the correct assignment of N values is made to the sequence of exciton transition energies, they represent a particularly unique and precise data set to examine the envelope-function method of calculating subband edges and, in so doing, to deduce exciton binding energies for quantum-well widths in the range 17–70 Å.

We have now studied the photoluminescence and excitation spectra from a second wafer whose quantum wells were produced using growth interruption at the heterointerfaces. The heavy- and light-hole exciton transitions observed in this wafer confirm and extend the original data set. Furthermore, the band gap of the barrier layers in both wafers was directly observed by excitation spectroscopy. Thus errors caused by determining the barrier band gap from the Al-to-Ga composition ratio of the barrier are eliminated.

With widths corresponding to integral multiples of GaAs monolayers and the barrier-material band gap directly measured, the envelope-function calculations for this data set are tightly constrained. In addition, some 40 measurements in the literature now indicate that the conduction-band-offset fraction lies in the rather small range 0.64±0.06. Also, the effective masses of the carriers are quite accurately determined by low-temperature, bulk-crystal measurements. The envelope-function analysis is also tightened by the recent finding[3] that nonparabolicity causes an almost negligible role in determining the lowest quantum-well subband-edge regardless of its energy.

A comparison of the sum of subband-edge energies in the conduction and valence bands, so calculated, with the exciton transition energies (by which we mean the difference of photon energies and the GaAs band-gap energy of 1.5192 eV at ~ 6 K, i.e., $h\nu - E_g$) should yield the exciton binding energy. If the quantum-well potential is taken as a square well, we find that the deduced exciton binding energies decrease as the well width decreases from 60 to 30 Å before beginning the expected increase for still narrower wells. All theories of two-dimensional confinement of excitons show that such a dependence is physically unacceptable. We conclude that a potential well having smooth, rather than abrupt, edges must be used to model very narrow quantum wells. This is supported by the recent work of Van de Walle and Martin[4] which shows that the transition to bulk-crystal properties occurs in a distance of about one monolayer on each side of a chemically abrupt interface.

The exciton binding energies deduced from the smooth-edge well calculation have the expected increase with decreasing well width. They can be compared to a few measurements of others[5,6] for well widths in the 60–75 Å range and to one measurement made in the present study on a 31-Å well from the $2s$-$1s$ splitting. These comparisons indicate that free charge screening has reduced the exciton binding energy by approximately 2.5 meV in our interrupted growth wafers. The unintentional doping, probably an acceptor from previous experience, must be in the barrier in order to give free charge in the well at low temperature and need be only at a level of 1×10^{14} cm^{-3}, a very small value.

The exciton binding energies that we deduce are found to rise to approximately 25 meV for a well width of 17 Å, an exceptionally large value. We find, however, that the exciton binding energies we observe by excitation

spectroscopy in the barrier are close to this value, and they should be regarded as intercept values in the limit of zero well width. The recent work of Pearah *et al.*[7] also observed exceptionally large exciton binding energies in bulk $Al_xGa_{1-x}As$ crystal for $0.35 \lesssim x \lesssim 0.45$, thus giving further support to the deduced values.

II. EXPERIMENTAL PROCEDURES

The two wafers on which measurements were made were grown in a nominally identical manner by molecular-beam epitaxy at 600 °C on a rotating substrate holder with a two-minute interruption at each heterointerface.[1] A 5000-Å GaAs buffer layer was grown on a (100) semi-insulating GaAs substrate followed by 1000 Å of $Al_{0.40}Ga_{0.60}As$, then GaAs wells of nominal widths of 100, 50, 25, and 15 Å, each separated by 300-Å $Al_{0.40}Ga_{0.60}As$ barrier layers, and finally a top layer of 1000 Å of the same alloy. Evidence of well widths equal to integral numbers of GaAs monolayers was found only for the nominally 50-, 25-, and 15-Å wells with several well widths arising from each nominal well width and caused by variations across the wafer.[2] For the nominally 100-Å-width well only a single heavy-hole exciton peak and a single light-hole exciton peak were observed, we believe, because the frequency width of the transitions from successive integral number of monolayer wells exceeded their separation.

Various characteristics of the low-temperature ($\sim$6-K) photoluminescence and excitation spectra of wafer 1 were discussed earlier.[1] Typical spectra are exhibited there.[1] Those of wafer 2 are qualitatively similar, the only differences being slightly wider wells and a slightly lower-barrier band gap.

Table I lists the observed transition energies $h\nu - E_g$ from both wafers. The transition energies are those observed from excitation spectra, that is, from absorption peaks except for those for $N=8,9$ in wafer 1 and $N=9,14$ in wafer 2. These were seen only in photoluminescence where the thermal population factor in emission overcomes the very weak strength brought about by the rare occurrence of that well width in the excitation volume. They were corrected upward respectively by 1.2, 0.8, 1.3, and 0.3 meV for Stokes shifts as determined from direct comparisons of spectral positions of emission and absorption in neighboring transitions. The monolayer assignments are also shown in Table I. Those for wafer 1 are greater by one than the original, tentative assignments.[1] The assignments are quite certain. For example, if the monolayer assignments for the sequence of transitions assigned to $N=6-13$ in wafer 1 were lowered by one, unacceptably high exciton binding energies of approximately 50 meV would result for $N=5$, while if the assignments were raised by one, negative exciton binding energies would result.

The well width corresponding to the monolayer number in Table I is based on a monolayer thickness of GaAs (one half the lattice parameter) being 2.8237 Å at approximately 6 K. This is obtained from the lattice parameter[8] of 5.653 25 Å at 300 K and integration over temperature of its thermal-expansion coefficient.[9] Figure

TABLE I. Heavy (hh) and light (lh) hole exciton transition energies $h\nu - E_g$ observed in wafers 1 and 2 vs the monolayer number and the corresponding well width in Å. Calculated values of the sum of subband-edge energies of the conduction band and heavy- or light-hole valence bands are also listed. The soft-edge well and screening corrections are explained in the text. Deduced exciton binding energies B_{ex} are also listed. All energies are in meV.

Monolayer number	Well-width (Å)	$h\nu - E_g$ wafer No. 1		Subband-edge calc		$h\nu - E_g$ wafer No. 2		Subband-edge calc		Smooth-edge well corr		Screening corr $p = 3\times10^8$ cm^{-2}		B_{ex} from No. 1		B_{ex} from No. 2	
		hh	lh	hh	lh	hh	lh	hh	lh	hh	lh	hh	lh	hh	lh	hh	lh
6	16.942	298.5	333.8	314.6	350.4					7.2	5.0	2.8	2.7	26.1	24.3		
7	19.766	273.7	309.6	283.7	321.4	267.8	302.8	280.9	317.3	7.1	5.0	2.8	2.7	19.9	19.5	23.0	22.2
8	22.590	246.4		256.5		242.8	279.8	254.0	291.4	6.6	4.9	2.8	2.7	19.5		20.6	19.2
9	25.413	224.7		232.4		221.7		230.4		6.0	4.7	2.7	2.6	16.4		17.4	
10	28.237	203.4		211.3						5.5	4.4	2.7	2.6	16.1			
11	31.061	185.3	221.2	192.8	230.0					5.0	4.1	2.6	2.5	15.1	15.4		
12	33.884	169.5	203.9	176.4	212.6	167.5	202.0	175.2	210.6	4.5	3.8	2.6	2.5	14.0	15.0	14.8	14.9
13	36.708	155.8		162.0		154.3	187.8	160.9	195.1	4.0	3.5	2.6	2.5	12.8		13.2	13.3
14	39.532					142.6		148.2		3.6	3.2	2.6	2.5			11.8	
20	56.474	88.0	112.7	96.3	122.3					2.1	2.0	2.6	2.4	13.0	14.0		
21	59.298	82.4	106.2	90.3	115.1					2.0	1.9	2.5	2.4	12.4	13.2		
22	62.121	77.3	99.8	84.7	108.7					1.8	1.7	2.5	2.4	11.7	12.9		
23	64.945	73.0	93.8	79.7	102.5					1.7	1.6	2.5	2.4	10.9	12.7		
24	67.769					67.2	86.8	74.8	96.4	1.6	1.5	2.5	2.4			11.7	13.5
25	70.593					63.5	82.8	70.6	91.3	1.5	1.5	2.5	2.4			11.1	12.4

1 is a plot of the transition energies of both heavy- and light-hole excitons versus the assigned monolayer number.

In order to further constrain the calculation of subband edges we measured the band gap of the barrier material directly by extending the excitation range. The heavy and light excitons of the $Al_xGa_{1-x}As$ barrier material, split by the small amount of lattice-mismatch strain, were observed. Both the 1s ground states and the 2s excited states were resolved. Multiplying the 2s-1s splitting by $\frac{4}{3}$ give the exciton binding energy in each case and determines the band gaps between the conduction and the heavy- and light-hole valence bands in the strained material. In wafer 1 the heavy- and light-hole exciton binding energies in the barrier were found to be 25.2 and 22.9 meV and in wafer 2 to be 25.5 and 21.3 meV. In wafer 1 the barrier band gaps with respect to the heavy- and light-hole valence bands were found to be 2.0133 and 2.0190 eV and in wafer 2 they were found to be 2.0047 and 2.0089 eV. Further analysis of these and similar measurements will be published elsewhere.

Exciton-binding-energy measurements for the well-confined excitons by the 2s-1s splitting method[6,10] are not in general possible in our two interrupted-growth wafers because excitons from several well widths differing by a monolayer each are usually observed at once. However, in one case for an exciton assigned to $N=11$ ($l=31.061$ Å) the 2s-state edge was visible as shown in Fig. 2. Taking the 2s-state energy as halfway up the edge[10] (see arrow on left in Fig. 2) and dividing by 0.87, as derived in Ref. 10, yields a heavy-hole exciton binding energy of 13.1 meV. If the 2s-state energy is chosen at the top of the rise as done in Ref. 6 (see arrow on right in Fig. 2) and the 2s-state binding energy of 1.9 meV (Ref. 6) is added to the 1s-2s splitting, a heavy-hole exciton binding energy of 14.9 meV results. Since the observation of a spectral peak in Ref. 6 makes the binding-energy determination there more reliable than those of Ref. 10, and since the values found in Ref. 6 are larger than those in Ref. 10, the value of 14.9 meV is thought to be more reliable. This value aids in constraining the exciton binding energies deduced below from subband-edge calculations. It should be noted in Fig. 2 that the valley between the 1s and 2s states is not as pronounced as in the spectrum of Dawson *et al.*[6] The 2s peak-to-valley ratio in their work is 8:1 while it is only 1.6:1 in Fig. 2. Further, their 2s peak is a distinct peak while that of Fig. 2 is only an edge. The likely explanation for the lack of a distinct 2s peak in Fig. 2 is the presence of some free charge in the well resulting from unintentional doping of the barriers, which from past experience is likely to be an acceptor. Experience has also shown that growth interruption as used in our wafers tends to add additional carbon acceptors in the interface region. The presence of free charge in the wells is also indicated by the deduction of exciton binding energies in Sec. III.

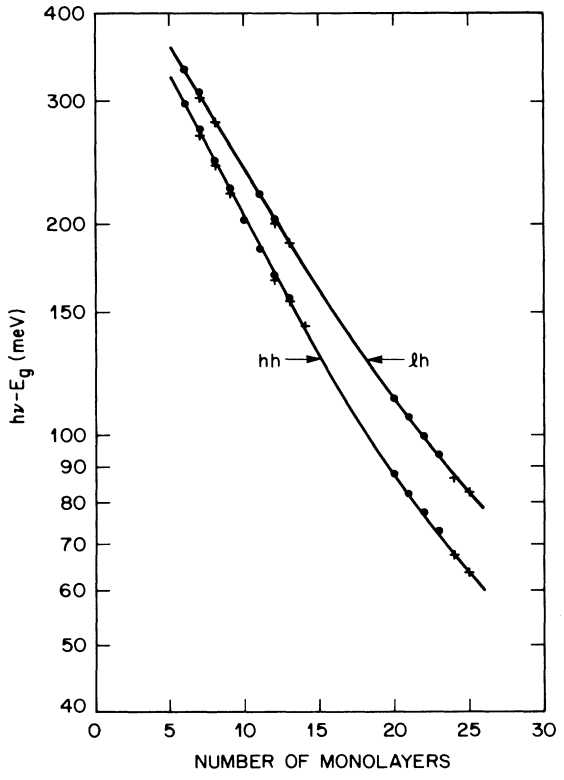

FIG. 1. Plot of heavy-hole (hh) and light-hole (lh) exciton transition energies vs the quantum-well width expressed in the number of monolayers of GaAs. The circles represent data from wafer 1 and pluses represent data from wafer 2. The curves are empirical.

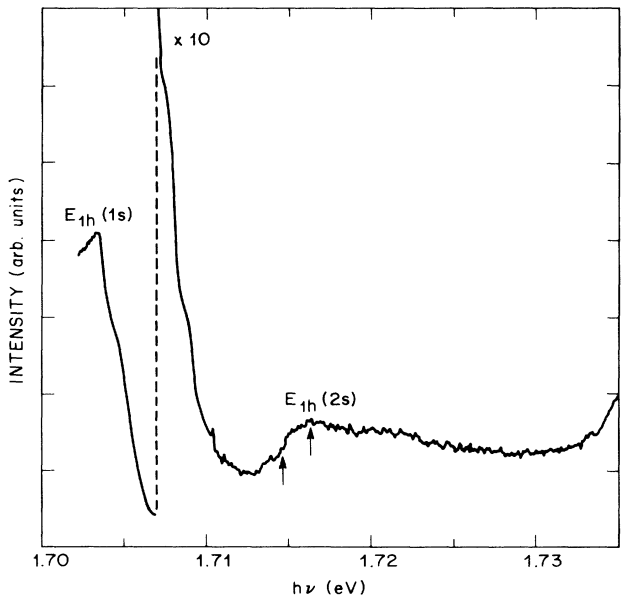

FIG. 2. Photoluminescence excitation spectrum of the ground 1s state and the excited 2s state of the heavy-hole exciton in an eleven-monolayer ($l=31.061$ Å) well. See text for meaning of arrows.

III. ENVELOPE-FUNCTION CALCULATIONS

If reliable exciton binding energies are to be obtained from the difference between the transition energies of Fig. 1 and the sum of the subband edges (quantum confinement energies) in the conduction and valence bands, the calculation of the subband edges using the envelope-function approach must involve only tightly constrained parameters. These parameters include well widths, band gaps of well and barrier materials, the offset parameter, masses, nonparabolicities, and the well shape. We discuss each of these in order.

The uniqueness of the present data stems from the exciton transition energies being associated with wells whose widths differ by one monolayer. Of course, widths differing by one monolayer means only that they are expressible as $(N+F)a$, where N is an integer, F a fraction of one (independent of N), and a is the GaAs monolayer thickness. Since both the well and barrier materials have planes of As atoms perpendicular to the growth direction [001], it is not immediately obvious that $F \cong 0$. However, the work of Van de Walle and Martin[4,11] shows that the edge of the well is at the center of the As layer and thus that $F=0$ is true to a high degree of accuracy. Thus, we assign well widths to integral multiples of the monolayer thickness. Since, as pointed out in Sec. II, a shift from the assigned integer in Table I and Fig. 1 by one leads to unacceptable or unphysical values of the exciton binding energies, the assigned well widths of Na have essentially no uncertainty in them.

In contrast to most work on quantum wells the barrier band gap was directly observed and accurately determined in this work. We observed by excitation spectroscopy the $1s$ and $2s$ states of the heavy- and light-hole excitons, split by the small lattice-mismatch strain, in the barrier. That allowed deduction of the exciton binding energies in the barrier and thus the different energy gaps between the conduction band and the light- and heavy-hole valence bands, whose values are quoted in Sec. II. By observing the barrier exciton states with the photoluminescence detector set successively on the heavy-hole exciton peak emitted from each well, the barrier band gap related to heavy and light holes in each wafer was found to be uniform to ± 1 meV throughout the epitaxial layers. The two barrier band gaps are used directly in the envelope-function calculation. However, they can be used to calculate the AlAs mole fraction x of the barrier through the formula $E_g(x)=1.5192+1.425x-0.9x^2+1.1x^3$ (Ref. 12). This indicates that wafer 1 had $x \cong 0.40$ (slightly different from $x=0.37$, quoted earlier[1]) and wafer 2 had $x \cong 0.39$.

The offset parameter Q_e, which determines the fraction of the difference of barrier and well band gaps occurring as a conduction-band discontinuity, has been measured some 40 times now in the $Al_xGa_{1-x}As/GaAs$ system. Those many measurements can be characterized as $Q_e=0.64\pm0.06$. We allow variation of Q_e only within this range when fitting the data to Fig. 1; we find $Q_e=0.70$ to be best.

Calculation of the subband-edge energies requires values of the electron, heavy-hole, and light-hole effective masses both in the well (GaAs) and in the barrier ($Al_xGa_{1-x}As$). The values we use in the well are, respectively, $m_e=0.0665$, $m_{hh}=0.34$, and $m_{lh}=0.094$ in units of the free-electron mass, values used before[13] in fitting a large set of quantum-well data. They each fall within the uncertainty interval of the best low-temperature bulk measurements: $m_e=0.066\,50 \pm 0.000\,07$ (Refs. 14 and 15), $m_{hh}=0.38\pm0.06$ (Refs. 16 and 17), and $m_{lh}=0.091\pm0.003$ (Refs. 16 and 17). It is worth noting that there is justification for increasing the light-hole mass a few percent above the bulk value. Sanders and Chang[18] showed that heavy- and light-hole band mixing for nonzero wave vectors k_p of in-plane motion produces a negative effective mass for the lowest light-hole band at $k_p=0$ and band minima for $k_p \neq 0$ that are approximately 2% lower than the $k_p=0$ value for a 50 Å-wide, $x=0.25$. Thus, the light-hole mass, which in the envelope-function approach predicts the $k=0$ subband intercept, must be increased approximately 4% to predict the subband edge. The tightness of the bulk uncertainty interval constraints is seen from the effective-mass changes of $\Delta m_e=\pm0.0009$ (1.3%), $\Delta m_{hh}=\pm0.013$ (3.8%), and $\Delta m_{lh}=\pm0.002$ (2.3%) needed to produce a subband-edge energy change of $\Delta E=\mp0.5$ meV for the $N=22$ well.

Since effective-mass measurements typically have not been made for the particular alloy composition used in the barrier, interpolation between values for GaAs and AlAs is necessary. In the past this interpolation typically has been taken linear in the AlAs mole fraction x. However, from band theory of III-V semiconductors it is known that an effective mass is proportional to an effective energy gap which is rather close in value to the direct gap, while the direct gap often is a nonlinear "bowing" function of the mole fraction x. Thus, it should be more accurate to interpolate effective-mass values in the alloy by

$$m(\text{alloy})=m(\text{GaAs})+[m(\text{AlAs})-m(\text{GaAs})]f \ , \tag{1}$$

where

$$f \equiv [E_g(\text{alloy})-E_g(\text{GaAs})]/[E_g(\text{AlAs})-E_g(\text{GaAs})] \ . \tag{2}$$

This interpolation method has the further advantage of using only the directly measured barrier band gap $E_g(\text{alloy})$, which is found to be slightly different for heavy and light holes, and the well-known values of E_g for GaAs and AlAs given in the $E_g(x)$ formula earlier in this section.

Reliable experimental data on effective masses in AlAs are sparse. Thus, it appears that theoretically derived values are most reliable. We use $m_e=0.15$ (Ref. 19), $m_{hh}=0.40$ (Ref. 20), and $m_{lh}=0.18$ (Ref. 20). Though there is greater uncertainty in their values than those for GaAs, there is also considerably less sensitivity to their values because of the interpolation for an alloy of approximately $x=0.40$ and because they affect only that portion of the wave function which penetrates the barrier. Thus, changes of $\Delta m_e=\pm0.0074$ (4.9%),

$\Delta m_{hh}=\pm 0.16$ (40%), and $\Delta m_{lh}=\pm 0.015$ (8.4%) are necessary to produce a subband-edge energy change of $\Delta E=\mp 0.5$ meV for the $N=22$ well.

We include nonparabolicity by an empirical two-band model[3] applicable to quantum wells. It is based on Bastard's derivation of the envelope-function approximation for two-[21] and three-band[22] interaction models, but with an altered interpretation of the parameters. The model can be expressed in an energy-dependent effective-mass form. For a single, square quantum well it consists of the dispersion relation in the well

$$E=\frac{\hbar^2 k_w^2}{2m_w(E)} , \tag{3}$$

the dispersion relation in the barrier

$$E=V-\frac{\hbar^2 k_b^2}{2m_b(E)} , \tag{4}$$

and the combination of boundary conditions

$$\left[\frac{k_w m_b(E)}{k_b m_w(E)}-\frac{k_b m_w(E)}{k_w m_b(E)}\right]\tan(k_w l)=2 . \tag{5}$$

Here the subscripts w and b denote well and barrier, the wave numbers k_w and k_b are both real numbers corresponding to wave functions having trigonometric functions in the well and exponentially decaying functions in the barriers, l is the well width, V is the energy height at the interfaces [$Q_e\Delta E_g$ for the conduction band and $(1-Q_e)\Delta E_g$ for the valence band where $\Delta E_g=E_g(\text{alloy})-E_g(\text{GaAs})$], and the energy-dependent effective masses are given by

$$m_w(E)=m_w(1+E/E_w) , \tag{6}$$

$$m_b(E)=m_b[1-(V-E)/E_b] , \tag{7}$$

where E_w and E_b are the effective energy gaps in the well and barrier materials that represent an appropriately weighted position of all the bands that interact to produce that particular effective mass. The usual nonparabolicity parameter γ is related to the effective energy gap and the effective mass by

$$\gamma_i=\frac{\hbar^2}{2m_i E_i} \quad (i=w,b) . \tag{8}$$

The model also relates these properties on the two sides of the interface by

$$m_w/m_b=E_w/E_b , \tag{9}$$

$$\gamma_w/\gamma_b=(m_b/m_w)^2 . \tag{10}$$

In the empirical two-band model we regard m_w, m_b, and γ_w as adjustable parameters, that is, parameters which can be set independently to experimental values. The model can be applied to any band: conduction, heavy-hole valence, or light-hole valence band.

The surprise of this model[3] of nonparabolicity is that the nonparabolicity shift of a quantum-well subband-edge energy does *not* depend simply on the subband edge having a large energy. It *must* also have a large occupancy probability in the well as distinct from the barriers. This means that high nonparabolicity lowering of subband edges occurs only for high-quantum-number subband edges. For the lowest subband edge, even when at a high energy, the effect is always minute ($\lesssim 1$ meV) and, contrary to expectations, is always a raising of the subband-edge energy.

For the above reasons the nonparabolicity parameter values, $\gamma_e=4.9\times 10^{-19}$ m^2 and $\gamma_{lb}=7.4\times 10^{-19}$ m^2 calculated from a five-band interaction model,[13] are completely adequate. Since the nonparabolicity of the heavy-hole band is an order of magnitude or so below the above values, it can be adequately taken as zero.

With the parameters now fixed, the envelope-function model can be used to calculate the lowest subband-edge energy for electrons, heavy holes, and light holes. The sum of those for electrons and heavy holes (or light holes) can be compared to the heavy- (or light-) hole exciton transition energies $h\nu-E_g$(GaAs) in columns 3 and 7 (or 4 and 8) of Table I. Because the interrupted-growth technique produces wells that are chemically abrupt, it is natural to attempt to model the well potential as a square well as used for Eqs. (3)–(5). Calculated energies for a square well are given in columns 5, 6, 9, and 10. The difference between these and the corresponding exciton transition energies of columns 3, 4, 7, and 8 should be the exciton binding energies. We find, however, that the exciton binding energies found from this difference decrease in going from 60- to 30-Å well widths before a sharp rise occurs for narrower wells. A minimum in the exciton binding energy function is inconsistent with expectations of confinement of quasi-two-dimensional excitons.

We attribute this discrepancy to the use of the idealized square well. If the well edges are smooth, rather than abrupt, the lowest subband edge is expected to be raised with the amount of raising larger for narrower wells. The work of Van de Walle and Martin on strained layer Si/Ge heterointerfaces[4] and on GaAs/AlAs (100) heterointerfaces[11] supports such a smooth transition of the potential with the transition distance being close to one monolayer (100) on both sides of the chemically abrupt heterointerface. Thus, we are led to model the well by

$$V(z)=\begin{cases} V+\dfrac{V_0}{2}\left[-1+\tanh\left[\dfrac{z-Na/2}{a}\right]\right] & (z\geq 0) , \\ V+\dfrac{V_0}{2}\left[-1-\tanh\left[\dfrac{z+Na/2}{a}\right]\right] & (z\leq 0) , \end{cases} \tag{11}$$

where

$$V_0=V/[1+N^{-1}\ln(1+e^{-N})] . \tag{12}$$

Here a is the width of a monolayer, N is the integral number of monolayers, V_0 is determined by Eq. (12) to make $\int_{-\infty}^{\infty}[V-V(z)]dz=NaV$, and the zero of potential is the band edge of the well. This potential well is illustrated in Fig. 3. The additional energy that this po-

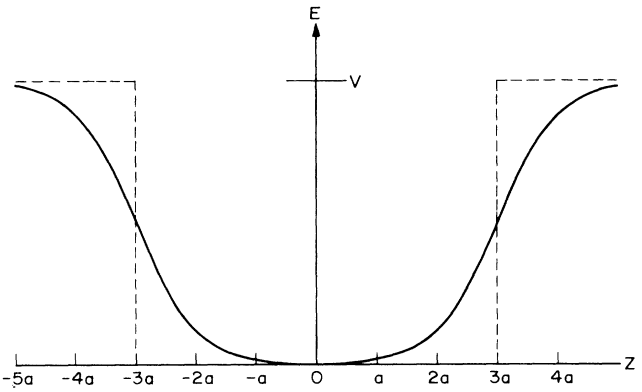

FIG. 3. Soft-edge-well profile representing Eqs. (11) and (12) for a six-monolayer-wide well, the narrowest well studied.

tential gives the sum of lowest electron and heavy- (or light-) hole subband edges is shown in Fig. 4 and listed in column 11 (or 12) of Table I. As seen from the data of Table I, the use of this potential eliminates the minimum in the deduced exciton binding energies around 30-Å well widths. A change of the transition length parameter by $\pm a/3$ causes a change of ± 1 meV for $N=22$ and ± 3 meV for $N=6$ for both heavy- and light-hole exciton binding energies.

IV. EXCITON BINDING ENERGIES

Subtraction of the observed exciton transition energies from the sum of the subband-edge energies calculated with the smooth-edge potential gives the exciton binding energies present in our interrupted-growth wafers. They can be compared to two recent and reliable measurements of exciton binding energies in the 60–75-Å well-width range. They are the 12.1-meV heavy-hole exciton binding-energy measurement at 75 Å and $x=0.40$ of Dawson *et al.*[6] and the 12.5±1-meV and 13.5±1-meV measurements of the heavy- and light-hole exciton binding energies at 60 Å and $x=0.35$ of Rogers *et al.*[5] This comparison indicates the values for both heavy- and light-hole exciton binding energies deduced here are about 2.5 meV low in this well-width range.

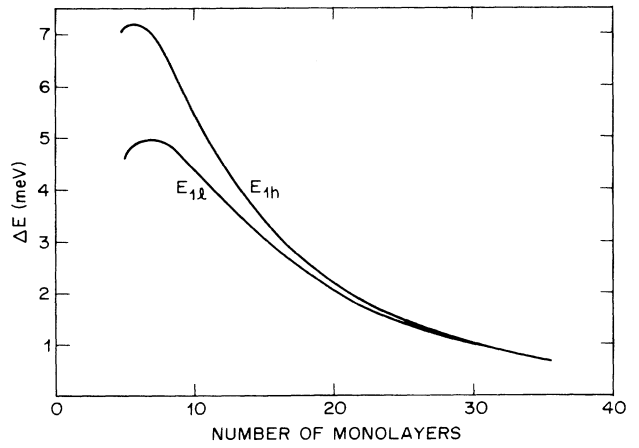

FIG. 4. The increase of energy of the heavy-hole exciton E_{1h} and the light-hole exciton E_{1l} from subband-edge energy changes arising from the soft-edge well relative to the square well ($x=0.40$, $Q_e=0.70$).

We attribute this discrepancy to a small amount of free charge in the well resulting from unintentional doping, probably an acceptor, in the barrier layers or particularly at the heterointerfaces because of the interrupted-growth technique. This hypothesis is supported by the lack of a distinct $2s$-state peak in Fig. 2 and the low $2s$ peak-to-valley ratio shown there.

Both Kleinman[23] and Sanders and Chang[18] calculated the reduction in exciton binding energies as a function of free charge density (either holes or electrons) and well width. They found the binding energies to be very sensitive functions of the charge density. The work of Sanders and Chang shows that an areal density of only 3×10^8 holes/cm^2 can lower both heavy- and light-hole binding energies by about 2.5 meV in the 60–70-Å well-width range. For such a low charge density the binding-energy reduction is only a slow function of well width, as can be seen from columns 13 and 14 of Table I. Since the $Al_{0.4}Ga_{0.6}As$ barriers between the wells are 300 Å wide, the unintentional doping of the barriers would be only 1×10^{14} acceptors/cm^3, a value that cannot be ruled out because it is 10–30 times less than has been observed in other samples grown in the same apparatus. We thus believe it reasonable to hypothesize its presence.

Additional support for the 2.5-meV reduction comes from our heavy-hole exciton binding-energy measurement in wafer 1 shown in Fig. 2. That measurement gave 14.9 meV for $N=11$ ($l=31.061$ Å).

On the basis of these several reasons we add the screening corrections of columns 13 and 14 of Table I to the binding energies to obtain the final results listed in columns 15–18 for the two wafers. They are also plotted in Fig. 5. The measurements of Dawson *et al.*[6] and Rogers *et al.*[5] and our $2s$-$1s$ measurements at $l=31$ Å are also plotted for comparison. The curves are simply smoothed representations of the data.

The deduced exciton binding energies show a monotonic increase as the well width decreases in the measurement range, the effect of increasing two-dimensional confinement. For the narrowest three well widths studied the binding energy for the light-hole exciton is found to be less than that for the heavy-hole exciton, the reverse of the relationship at wider well widths. This crossover of the exciton binding energies is expected from the greater penetration of the light-hole exciton wave function into the barrier and from the lower light-hole exciton binding energy found in the barrier material. Each exciton binding energy is expected to reach a maximum determined by an interplay of increasing two-dimensional confinement and increasing penetration of the barriers by the exciton wave function. This apparently occurs at a well width smaller than the six monolayers (16.942 Å) of our narrowest well and is shown schematically by the dashed portions of the

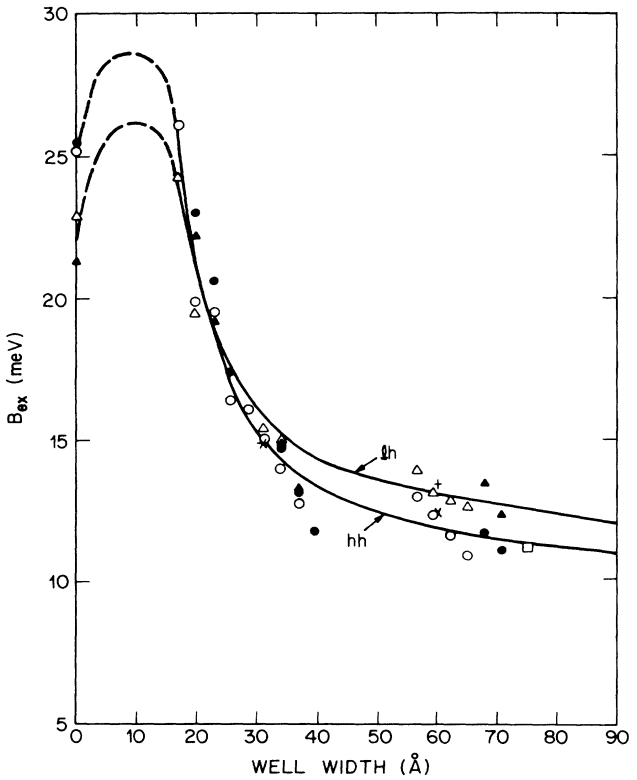

FIG. 5. Heavy-hole (hh) and light-hole (lh) binding energies B_{ex} vs the well width; open circles and triangles for hh and lh of wafer 1, solid circles and triangles for hh and lh of wafer 2, a square for hh from Dawson *et al.* (Ref. 6), a cross and a plus for hh and lh from Rogers *et al.* (Ref. 5), a star for our hh $2s$-$1s$ measurement in wafer 1, and points at zero well width for our barrier-layer measurements. The curves are empirical; the dashed portions are only schematic.

curves. As the well width approaches zero, the exciton binding energies should approach the exciton binding energies of the barrier material. As mentioned earlier, these were deduced from observations of the $2s$-$1s$ splitting of excitons in the barrier in both wafers and are plotted in Fig. 5 at zero well width. The heavy- and light-hole excitons remain split in the barrier due, we believe, to the small lattice mismatch of $Al_{0.4}Ga_{0.6}As$ to GaAs. In view of the large exciton binding energies in the barrier alloy, the large values reached for wells of six monolayers are not surprising. Large values of exciton binding energies in bulk alloy crystals, comparable to those found here, were recently reported by Pearah *et al.*[7] They found the exciton binding energy rose dramatically from 10.6 meV at $x=0.29$ to 39 meV at $x=0.44$. Their data indicate that exciton binding energies such as we present here should depend strongly on the barrier composition for very narrow well widths.

There is no straightforward method of determining the uncertainties in our deduced exciton binding energies. However, we indicated above the sensitivity of the calculated subband-edge energies to variations of the several carrier masses and to a variation of the transition width parameter in the smooth-edge potential. As pointed out earlier, the results have no significant sensitivity to the bulk nonparabolicity parameters. It is also worth noting that using the average value 0.64 of the 40 some recent measurements of the conduction-band-offset parameter Q_e, rather than 0.70, would cause the heavy-hole exciton energy at $N=22$ ($l=62.121$ Å) to drop by 1.5 meV and the light-hole exciton energy to rise by 0.9 meV. This would make the splitting between the two types of exciton binding energies unacceptably large at this well width when compared to the Rogers *et al.*[5] and Dawson *et al.*[6] data. Furthermore, use of $Q_e=0.64$ would lower the heavy-hole exciton energy by 5.6 meV and raise the light-hole exciton energy by 3.0 meV at $N=6$ ($l=16.942$ Å) and thus eliminate the expected crossover of exciton binding energies shown in Fig. 5. When all these sensitivities are considered, we estimate the uncertainties in the exciton binding energies to be about 2 meV for well widths near 60 Å rising to about 5 meV for well widths near 17 Å.

V. CONCLUSIONS

We used a unique data set of heavy- and light-hole exciton transition energies measured from a series of quantum wells produced by the interrupted-growth technique and having widths of integral numbers of monolayers of GaAs to test the envelope-function method of calculating subband-edge energies. The analysis was further constrained by direct measurements of the barrier band gap and the exciton binding energies in the barrier. Nonparabolicity was included by an empirical two-band interaction model[3] that shows that nonparabolicity plays an almost negligible role in determining the energy of the lowest subband edge in a quantum well regardless of the energy of that edge. We found the envelope-function approach is usable down to our narrowest well width of 17 Å provided a smooth-edge potential well, rather than a simple square well, is used. From the analysis and a comparison with a few recent and reliable exciton binding energies for narrow wells, we concluded that the binding energies in our wafers were reduced by 2.5 meV from screening by free charge originating from unintentional barrier doping at a level of 1×10^{14} cm^{-3}. After applying a correction to compensate for this screening, exciton binding energies were deduced down to well widths of 17 Å. The large exciton binding energies, approximately 25 meV, that we find at this well width are comparable to the exciton binding energies that we observe directly in the barrier layers.

ACKNOWLEDGMENTS

We wish to thank C. G. Van de Walle and R. M. Martin for furnishing us with unpublished plots of potentials and charge densities at the GaAs/AlAs(100) interface based on their theory[4] and for useful conversations about their work.

[1]R. C. Miller, C. W. Tu, S. K. Sputz, and R. F. Kopf, Appl. Phys. Lett. **49**, 1245 (1986).
[2]P. M. Petroff, J. Cibert, A. C. Gossard, D. J. Dolan, and C. W. Tu (unpublished).
[3]D. F. Nelson, R. C. Miller, and D. A. Kleinman, Phys. Rev. B **35**, 7770 (1987).
[4]C. G. Van de Walle and R. M. Martin, Phys. Rev. B **34**, 5621 (1986).
[5]D. C. Rogers, J. Singleton, R. J. Nicholas, C. T. Foxon, and K. Woodbridge, Phys. Rev. B **34**, 4002 (1986).
[6]P. Dawson, K. J. Moore, G. Duggan, H. I. Ralph, and C. T. B. Foxon, Phys. Rev. B **34**, 6007 (1986).
[7]P. J. Pearah, W. T. Masselink, J. Klem, T. Henderson, H. Morkoc, C. W. Litton, and D. C. Reynolds, Phys. Rev. B **32**, 3857 (1985).
[8]J. B. Mullin, B. W. Straughan, C. M. H. Driscoll, and A. F. W. Willoughby, in *Proceedings of the Fifth International Symposium on Gallium Arsenide and Related Compounds, Deauville, 1974,* IOP Conf. Ser. No. 24 edited by J. Bok (IOP, Bristol, 1975), p. 275.
[9]S. I. Novikova, Fiz. Tverd. Tela (Leningrad) **3**, 178 (1961) [Sov. Phys.—Solid State **3**, 129 (1961)].
[10]R. C. Miller, D. A. Kleinman, W. T. Tsang, and A. C. Gossard, Phys. Rev. B **24**, 1134 (1981).
[11]C. G. Van de Walle and R. M. Martin (private communication).
[12]R. Dingle, R. A. Logan, and J. T. Arthur, Jr., in *Proceedings of the Sixth International Symposium on Gallium Arsenide and Related Compounds, Edingburgh, 1976,* IOP Conf. Ser. No. 33a, edited by C. Hilsum (IOP, Bristol, 1977), Chap. 4, pp. 210–214.
[13]R. C. Miller, D. A. Kleinman, and A. C. Gossard, Phys. Rev. B **29**, 7085 (1984).
[14]G. E. Stillman, D. M. Larsen, C. M. Wolfe, and R. C. Brandt, Solid State Commun. **9**, 2245 (1971).
[15]J. M. Chamberlain, P. E. Simmonds, R. A. Stradling, and G. G. Bradley, *Proceedings of the Eleventh International Conference on the Physics of Semiconductors, Warsaw, 1972,* edited by M. Miasek (PWN-Polish Scientific, Warsaw, 1972), p. 1016.
[16]K. Hess, D. Bimberg, N. O. Lipari, J. K. Fischbach, and M. Altarelli, in *Proceedings of the Thirteenth International Conference on the Physics of Semiconductors, Rome, 1976,* edited by F. G. Fumi (North-Holland, Amsterdam, 1976), p. 142.
[17]D. Bimberg, in *Festkörperprobleme XVII, Advances in Solid State Physics,* edited by J. Treusch (Vieweg, Braunschweig, 1977), p. 195.
[18]G. D. Sanders and Y.-C. Chang, Phys. Rev. B **35**, 1300 (1987).
[19]D. J. Stukel and R. N. Euwema, Phys. Rev. **188**, 1193 (1969).
[20]P. Lawaetz, Phys. Rev. B **4**, 3460 (1971).
[21]G. Bastard, Phys. Rev. **24**, 5693 (1981); **25**, 7484 (1982).
[22]G. Bastard, in *Molecular Beam Epitaxy and Heterostructures,* edited by L. L. Chang and K. Ploog (Martinus Nijhoff, Dordrecht, 1985), p. 381.
[23]D. A. Kleinman, Phys. Rev. B **32**, 3766 (1985).